Understanding Extensibility of Paper: Role of Fiber Elongation and Fiber Bonding

Jarmo Kouko (VTT Technical Research Centre of Finland Ltd), **Tuomas Turpeinen (**VTT Technical Research Centre of Finland Ltd), **Artem Kulachenko (**KTH Royal Institute of Technology, Sweden), **Ulrich Hirn** ([1]Graz University of Technology, [2] CD Laboratory for Fiber Swelling and Paper Performance, Austria), **Elias Retulainen (**VTT Technical Research Centre of Finland Ltd)

ABSTRACT

The tensile tests of individual bleached softwood kraft pulp fibers and sheets, and micromechanical simulation of fiber network suggest that only a part of the elongation potential of individual fibers is utilized in the elongation of sheet. The stress-strain curves of two actual individual pulp fibers and one classic fiber were applied to a micromechanical simulation of random fiber networks. Both the experimental results and the micromechanical simulations indicated that fiber bonding has an important role not only in determining the strength but also the elongation of fiber networks. Additionally, the results indicate that the shape of the stress-strain curve of individual pulp fibers may have significant influence on the shape of the stress-strain curve of a paper sheet. A large increase in elongation and strength of paper can be reached only by strengthening fiber-fiber bonding, as demonstrated by the experimental handsheets with starch and cellulose microfibrils and by the micromechanical simulations. The key conclusion related to this investigation was that simulated uniform inter-fiber bond strength does not influence the shape of the stress-strain curve of the fiber network until the bonds fail, whereas the number of bonds has an influence on activation of the fiber network and on the shape of stress-strain curve.

INTRODUCTION

Properties of individual pulp fibers play a pivotal role in the development of the mechanical properties of fiber networks and structures. Fiber strength determines the ultimate strength of paper and composite materials. However, the elongation potential of fiber networks is governed by the behavior of single fibers, inter-fiber bonding [1] and the network properties [2]. Reviews of strength and extensibility of single fibers and the papermaking potential of fiber networks are available [1-4]. High extensibility is a key material property for several paper packaging applications, e.g., paper sacks, paper cups or food trays. In this work, mechanical treatments were applied on commercial bleached softwood kraft pulp (BSKP) fibers, and the corresponding handsheets and simulated fiber networks were studied in order to increase understanding of the extensibility of this type of material.

There are several studies on the tensile properties of pulp fibers [5-16]. Typically, tensile strength and also elastic modulus are reported but strain at break is often disregarded. When stress-strain curves of individual restrained dried fibers are presented [10-11, 15 17-22], they are typically practically linear or slightly concave downward, with an elongation to break of about 2-6%. Significantly higher elongation values (~20%) have been reported for Longleaf pine fibers cooked in laboratory conditions and dried under longitudinal compression [23], for commercial Southern pine kraft pulp fibers dried individually on a Teflon treated glass plate allowing drying shrinkage [10], and for Loblolly pine fibers selected from the 5th annual ring at a low height of the tree [15, 22]. Due to the small length and width (0.7-3 mm length, 15-50 μm width) handling, mounting, and mechanical testing of individual pulp fibers is complicated and laborious. In this work, the stress-strain curves of individual BSKP fibers from a recent study [23] were applied in micromechanical simulations of fiber networks.

Mechanical treatment of pulp has been shown to be an efficient way to improve the elongation of paper. Three mechanisms are responsible for this. Firstly, improving the strength of the fiber-fiber bonding also increases the extensibility and strength of the paper. Poorly bonded fiber networks fail before the full elongation potential of fibers is reached, whereas in well-bonded networks the fibers are under higher stress and are more strained before network failure. Secondly, the creation of dislocations and microcompressions of fibers introduced by refining [24-25] has also been identified as a cause for increased paper elongation. Thirdly, increased swelling and reduced axial stiffness have been named as causes of higher drying shrinkage and the consequent higher elongation of paper. In contrast to the general belief, which favors hydrogen bonding, a recent investigation of different pulp fiber bonding mechanisms and bonding energies proposed that Van der Waals bonds play the most important role in fiber network bonding [26].

In recent years, more and more complex numerical models, such as micromechanical simulation of fiber networks applying beam-to-beam contact, have become possible with reasonable effort [27-28]. The novelty of the numerical simulation model is that it may enable investigation in conditions that cannot be achieved or cannot be measured experimentally. In this investigation the simulation model based on finite element (FE) model by Kulachenko and Uesaka [29] was used to predict the extensibility of random pulp fiber networks, while certain parameters were altered beyond the limits possible in actual paper sheets. Additionally, the number of active broken bonds during the straining of the fiber network can be investigated with the numerical simulation model. The simulated fiber bonds were point-wise, beam-to-beam contacts, and the actual nature of the bonds was not considered.

The objective of this study was to investigate the effect of the tensile behavior of individual softwood fibers, especially on the extensibility of the papers and simulated fiber networks made from those pulps and fibers, respectively. Understanding the roles of fiber elongation and bonding is highly significant for the development of new fiber-based packaging products. We link the measurements performed on the individual fibers with the network behavior using the fiber level simulation tools. We reflect on the differences observed in the simulations and experiments performed on the sheets made of these fibers.

EXPERIMENTAL

Materials

Raw materials. The raw material was a dried bleached softwood kraft pulp (BSKP), a mixture of spruce and pine, from a Nordic pulp mill. The BSKP was refined at 40% solids content (high consistency, HC treatment) using a wing defibrator (WD) exactly according to [30]. WD is a high-intensity single stage batch wood chip refiner equipped with four rotating blades. Additional information on the refining conditions for HC treatment can be found [31]. The HC treatment was followed by Valley beating (LC treatment) according to the standard procedure (SCAN-C 25:76). HC treatment of BSKP is known to increase both small and large-scale fiber deformation, whereas LC treatment straightens the fibers without significantly removing small-scale deformations [1]. Fiber properties of the pulps were measured using the STFI FiberMaster (the fibers were measured in swollen state). The length weighted (LW) average fiber lengths and widths, as well as the shape factors, are presented in Table I.

Table I Average fiber and pulp properties.

	Untreated	HC+LC
Length weighted fiber length of pulp, mm (FiberMaster)	1.83	1.80
Length weighted fiber width of pulp, μm (FiberMaster)	26.6	27.1
Shape factor, % (FiberMaster)	83.7	83.3
SR number (ISO 5267-1), -	12	25
WRV (ISO 23714), g/g	1.08	1.47

Paper sheets. The pulps were made into 60 g/m^2 handsheets according to EN ISO 5269-1. All handsheets were wet pressed at 350 kPa for 5 + 2 min with one exception, which is described later. Two drying methods were used to vary the shrinkage of the sheets: restrained drying after wet pressing according to the EN ISO 5269-1 and unrestrained drying between two forming wires that were supported by a grid and separated by a 5 mm thick rod. Untreated BSKP sheets were dried unrestrained and restrained, whereas HC+LC BSKP sheets were only dried unrestrained.

Additionally, high pressure wet pressing and addition of strength chemicals were applied in order to improve bonding of the fibers. A few untreated BSKP sheets were wet pressed using 670 kPa pressure (instead of 350 kPa) before unrestrained drying. Combination of 1.5% cationized starch, Cationic polyacrylamide (CPAM) 200 g/t and 5% Masuko micro-fibrillated cellulose (CMF) from VTT (E393HWM3) was added into untreated BSKP and the sheets were dried unrestrained and restrained. Detailed information of the applied chemicals can be found in [23]. Testing of the dry sheets took place at a temperature of 23 °C and at 50% relative humidity, using a strain rate of 10 mm/min (0.167 %/s) in a Lloyd tensile tester, in accordance with ISO 5270:2012.

Methods

Preparation of single fibers. Fibers for individual testing were prepared following the method described by Kappel et al. [32]. Dry pulp was dispersed and allowed to swell in water for at least 12 hours. The fibers were disintegrated according to DIN EN ISO 5263-1. A highly dilute suspension with a consistency of 0.01% was prepared. Small drops of the suspension were placed on a piece of Teflon foil (40 mm x 40 mm) and covered with another piece of Teflon foil. This sandwich was dried in a conventional sheet dryer for 45 minutes. The drying method used allowed shrinkage of the individual fibers. In order to perform single fiber tensile tests, the individual fibers were glued onto the sample holder (Fig. 1) using a two component epoxy resin (UHU PLUS ENDFEST). The sample holder used for the fiber tensile strength testing is described in [16, 33]. The gap in the sample holder was 0.5 mm. The span length is known to influence the strength [34]. After gluing of the individual fibers (Fig. 1), they were conditioned for at least 24 h prior to identification and testing to ensure the maximum holding strength of the resin and moisture equilibrium. The dry BSKP fibers were photographed before tensile testing and identified using a Leica DMLM microscope with 50x magnification and OptiMOS monochrome sensor camera from QImaging and using literature as a reference [35].

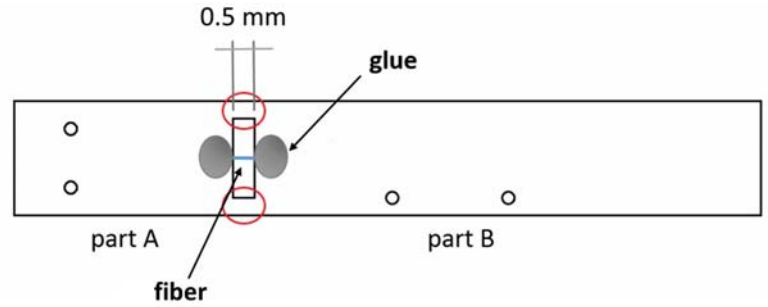

Fig. 1 Sample holder with 500 µm gap used for tensile testing

Single fiber tensile testing. The single fiber tensile testing was performed using the fiber bond tester at TU Graz [16, 33, 36]. Off-set force was measured prior to the test and then a minor preliminary loading was applied to fiber. A displacement measurement system (shown in Figure 2) was attached to the fiber bond tester in order to measure load-elongation data of the single fiber tensile tests. The displacement of the tension support was measured using a laser displacement sensor (Micro-epsilon OptoNCDT LD 1605-10, with a resolution of 3 µm). The displacement data was recorded using a National Instruments data logger system. The velocity of the moveable support of the fiber bond tester turned out to be very stable within the measurement accuracy of the laser sensor and therefore the linear fit of each measured displacement as a function of time was used in order to decrease the noise of the displacement data. The load data recorded by the fiber bond tester was complemented by the displacement data as a function of time in the data analysis afterwards. Both data were measured at 1 kHz frequency.

Sample holder mounting was performed as described by [16, 33]. The sample holder was placed under a light microscope, which was equipped with a digital camera [36] and a computer monitor. The tensile test was recorded with the imaging system, which enabled rejection of the tests in which gluing failed. The fibers were strained until break at 1 µm/s elongation speed (0.2%/s strain rate). The initial part of the force-strain curve was not recorded due to pre-tensioning of the fiber before the test. The initial strain that corresponded to the initial force was calculated using the initial slope (initial tangential modulus) of the force-elongation curve. All tests were performed in a climate room at 23°C temperature and 50% relative humidity.

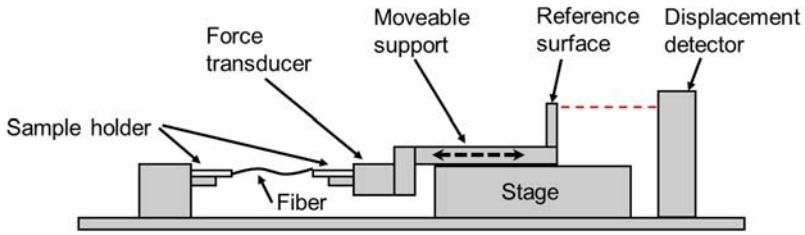

Fig. 2 Schematic image of the fiber bond tester with the laser displacement detection system

Fiber network simulation model. Deformation of 3D random fiber networks was simulated using the beam-based finite element (FE) model described in detail in the series of publications [37-39]. The FE model is capable of simulating the tensile behavior of a fiber network up to the failure point. The fibers are modeled as a series of a Timoshenko beam elements and the fiber bonds are represented through penalty-based beam-to-beam contacts. The model can exploit the stress-strain curve of an individual fiber, the number of active bonds and de-bonding properties in the fiber network, and the bond strength and stiffness in normal and shear directions. The limitation of the model is its inability to capture fiber failure.

The simulation networks were generated using a random deposition model that mimics the handsheet filtration process, i.e., the fibers fell on a flat surface and adjusted their shape according to the deposited fiber network. The process continued until the required grammage was reached. Wall thickness, diameter, length and curl of the fibers, and grammage and density profile of the network were the control parameters in the deposition model. An example of a deposited fiber network is presented in Fig. 3. As a result of the 3D FE simulation, the stress-strain curve of the fiber network, and the number of fractured and de-bonded contacts as a function of strain were obtained.

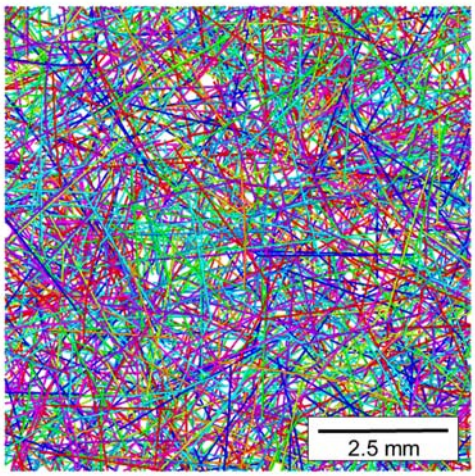

Fig. 3 A deposited fiber network for 3D FE simulation. Random colors were applied to the fibers in order to improve their visibility.

Simulation procedure. The FE simulation outputs the data readable by the commercial FE code. For the automatic simulation procedure, a Python code was applied to run a predefined sequence of the simulations. For each simulation case, 5-10 parallel network random realizations were simulated. The key parameters applied are presented in Table II. The length was varied according to Gaussian distribution, while the other fiber geometric parameters were set to a constant value. Admittedly, it does not fully correspond to the real case, where all the properties are subjected to non-Gaussian variations.

The key parameters including the stress-strain curves (see Fig. 4) of the actual fibers were obtained from the measurement of the individual BSKP fibers (a detailed description of the measurements is presented in [23]). The elongation of the individual BSKP fibers' stress-strain curves applied in the simulation was significantly higher (15% and 30%) compared to the typical elongation for similar fibers presented in literature. Additionally, the shape of the stress-strain curves of typical (classic-type) BSKP fibers presented in the literature are almost linear, whereas typically the stress-strain curves of the measured BSKP fibers were concave upward [23]. We used the multilinear plasticity with isotropic hardening to represent the curves in the simulation. In such an approach, the stiffness beyond the defined yield limit was taken as a tangent slope of the measured curve. The fiber straining during drying leads to straightening of the microfibrils and results in a linear behavior of the classic-type individual fibers [14]. The measured BSKP fibers were dried individually and drying shrinkage was not prevented, which is most probably the origin of the shape of the stress-strain curves. The non-linear shape of the fibers' response is the result of straightening of the kinks and the change in microfibril orientation angle (MFA) in the helical structure of the S2 layer. The change of the MFA is accompanied by the twist in case it is not inhibited by the boundary conditions [40]. The fibers in the experimental BSKP handsheets have probably experienced partly free and partly prevented drying shrinkage.

The simulations were made by applying stress-strain curves and fiber diameters for three kinds of fibers: Untreated-type BSKP, HC+LC-type BSKP and mimicked classic SW fibers (see Fig. 4). Table III presents characteristic properties of the BSKP fiber types applied in the fiber network simulation.

Paper chemicals have a limited possibility to increase the bond strength of an actual pulp fiber network (e.g., paper), whereas in simulations even infinite bond strength could be tested. The objective of the FE simulation was to investigate the influence of relative bond strength, relative number of active bonds and shape of individual fiber stress-strain curve on the stress-strain behavior of a simulated fiber network.

Table II The key parameters applied in the fiber network simulation.

Parameter	**Value**
Fiber length (Gaussian distribution)	2.5 mm (with St.Dev. of 0.5mm)
Fiber diameter	58 µm
Fiber wall thickness	4.4 µm
Cross-section shape	Elliptical (W/H ratio 2.9)
Grammage	60 g/m^2
Network dimensions	18 mm x 18 mm
Number of random realizations	10

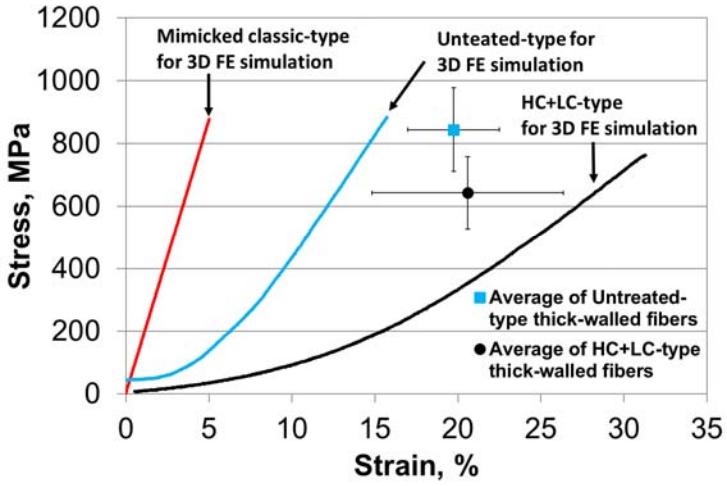

Fig. 4 Stress-strain curves of the thick-walled fibers: actual untreated BSKP, HC+LC treated BSKP, mimicked classic SW fiber with linear stress-strain behavior.

Table III The characteristic properties applied in the fiber network simulation.

Property (* = estimated)	Untreated-type thick-walled	HC+LC -type thick-walled	Mimicked classic thick-walled
Breaking force, mN	208	180	208*
Fiber width, µm	58*	58*	58*
Cross section area, µm^2	237	237	237*
Fiber thickness, µm	8.8*	8.8*	8.8*
Tangential modulus, GPa	8.0	4.0	17.5*

Since the point-wise contact is used in the simulations, the bond strength is defined in the force units. In this investigation, the unit shear bond strength was 10.9 mN (referred as 1x in this study) and the unit normal bond strength was a quarter of the unit shear bond strength (i.e., 2.7 mN). The simulated cases were 1x, 2x, 3x, 4x and 5x times the unit bond strength. Secondly, the relative number of active bonds varied from 20% to 100% with steps of 10%. The number of fiber bonds of deposited fiber networks was randomly removed in the model leaving the fiber network structure intact. The bond strength 10.9 mN applied in the simulations (referred as 1x) was slightly higher compared to the measured individual fiber bond strengths 4.6-8.5 mN presented in literature [41]. Because of the point-wise contacts, the detailed nature of fiber bonds should not be resolved explicitly. In reality, it has a significant role for actual papers affecting the strength of the bonds [26] and is the reason for the variation. A recent study showed that the relative contact area of pulp fiber bonds (apparent contact area/intersection area) may have a wide variation from 6.4% to 85% with an average of 57.7% [42]. In the simulations, however, the variations in the bond strength can be prescribed directly in the force units and can be varied across the network.

RESULTS

Strength properties of the actual individual BSKP fibers

The average values of investigated untreated and HC+LC treated BSKP fibers are presented in Table IV. The HC+LC treatments decreased the tensile strength of the thick-walled BSKP pulp fibers on average. Tensile strength in MPa units (force scaled with the cross-section area) of the BSKP fibers varied from 600 MPa to 840 MPa, which is comparable to the results obtained in other studies [10-12, 15]. As expected, a clear decrease in BSKP fiber strength was observed due to the mechanical treatments. The applied density of the fiber-wall for the actual measurement data was 1000 kg/m^3 according to [43-44].

Stress-strain curves of the individual thick-walled fibers are presented in Fig. 4. The markers with the 95% confidence intervals in Fig. 4 present average values of thick-walled fibers according to Table IV. The tensile curves of the individual BSKP fibers (Fig. 4) were concave upward. Increasing slopes may indicate the presence of dislocations or other fiber deformations, which were pulled straight during tensile testing. Large variation between the single BSKP fiber stress-strain curves in terms of shape, in addition to the variation of elongation from 10% to 32% was observed [23]. The individual fiber tensile curves presented in the literature have typically been apparently linear or slightly concave downward with elongation range from 3% to 6% [10, 15, 18-20, 22]. For that reason, the linear stress-strain curve was created for the mimicking behavior of classic SW fiber (shown in Fig. 4).

Table IV Average tensile properties and 95% confidence intervals of the individual BSKP fibers.

Property	Untreated thick-walled	HC+LC treated thick-walled
Breaking force, mN	235±37	145±26
Strain at break, %	19.7±2.8	20.6±5.8
Fiber width, µm	33.0±3.9	36.9±4.7
Cross section area, µm^2	280±30	230±30
Fiber thickness, µm	9.9±1.4	7.9±1.5
Tensile strength, MPa	840±130	640±120
Tangential modulus, GPa	6.5±1.5	5.2±0.8

Tensile properties of BSKP sheets

Tensile tests were performed for the BSKP sheets dried under restraint and without restraint. The tensile test results are presented in Table V and the stress-strain curves in Fig. 5 (a-b). There was a large difference in the tensile stiffness and elongation at break values between the restrained and unrestrained dried sheets. This can be attributed to the difference in drying shrinkage. Unrefined pulps gave the lowest strength and elongation at break values. Increased inter-fiber bonding by application of starch and cellulose microfibrils (CMF) and utilization of higher wet pressing pressure of the unrefined pulp improved elongation and tensile strength significantly. Applying LC refining to HC refined pulp increased both strength and elongation further. LC refining is known to make the fibers more straight and increase fiber swelling and subsequent shrinkage [29, 45].The HC+LC treatment in combination with unrestrained drying yielded the best elongation of 9.3% and tensile strength of 30 MPa of the studied BSKP samples. For unrestrained drying the stress-strain curves indicate that the increase in strain is more due to an increase in bonding and less to dislocations and other fiber deformations.

Table V Average tensile properties and 95% confidence intervals of the BSKP sheets.

	Untreated BSKP restrained	**Untreated BSKP unrestrained**	**HC+LC BSKP unrestrained**	**Untreated BSKP, starch, CMF restrained**	**Untreated BSKP, starch, CMF unrestrained**	**Untreated BSKP 6.7 kPa wet pressing unrestrained**
Tensile strength, MPa	13.6±0.5	6.4±0.2	30.0±1.8	21.0±0.8	17.5±2.1	12.3±0.7
Tensile index, Nm/g	25.2±0.9	15.2±0.5	53.1±2.3	40.6±1.5	37.2±4.2	24.6±1.4
Tensile modulus, GPa	2.21±0.11	0.86±0.04	1.09±0.03	2.03±0.16	1.02±0.05	1.21±0.06
Strain at break, %	2.12±0.18	3.02±0.18	9.25±0.26	3.65±0.30	6.2±1.1	4.76±0.18
Grammage, g/m^2	65.5	68.9	66.6	62.2	63.3	57.5
Density, kg/m^3	541	423	564	518	469	500

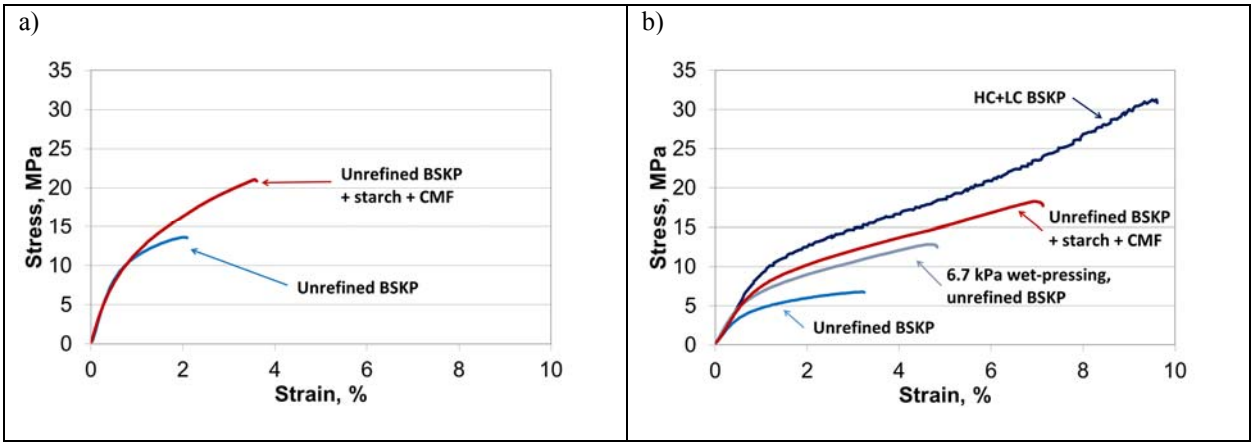

Fig. 5 Stress-strain curves of the actual BSKP handsheets with restrained (a) and unrestrained drying (b).

BSKP fiber network simulations

Influence of bond strength. The median stress-strain curves of simulated fiber networks with varied bond strength for untreated-type, HC+LC treated-type and mimicked classic SW fibers are presented in Fig. 6 a, c and e, respectively. Increase of bond strength from the reference value (1x) clearly increased the strength and elongation of the simulated fiber networks. The average strength and elongation of the simulated fiber networks with 95% confidence limits is presented in Figs. 6 b, d and, f. Interestingly, for the all simulated fiber types separately, the stress-strain curves of all the bond strengths fell exactly on the same curves, which is consistent with the earlier experimental [46] and numerical [47] studies showing the features of the stress-strain response of the network is mainly controlled by the fiber properties, while the network strength is influenced by the bond strength. The results indicate that fiber networks with uniform bond and fiber strength may have higher elongation than the individual fibers. More interestingly, a new random fiber network was deposited for each parallel simulation repeat. The relative tangent bond strength level 1x corresponds 10.9 mN has been applied in previous investigations [48-49]. However, up to 50-80 mN peak force has

been measured for intact individual fibers removed from a well-bonded paper sheet [50-51], but can be considered only as an indirect reflection of bond strength. Therefore, the simulated bond strength can be regarded as reasonable. The shape of the simulated untreated-type fiber networks was relatively similar to the stress-strain curves of the unrestrained dried handsheets shown in Fig. 5 b. The stress-strain curves of the simulated fiber networks of the untreated-type, HC+LC treated-type and mimicked classic SW fibers were different. The shape of the stress-strain curve of simulated untreated-type fiber network was similar to the classical stress-strain curves of sack paper. The results indicate that stress-strain curve of individual pulp fibers have an influence on the shape of the stress-strain curves of paper sheets.

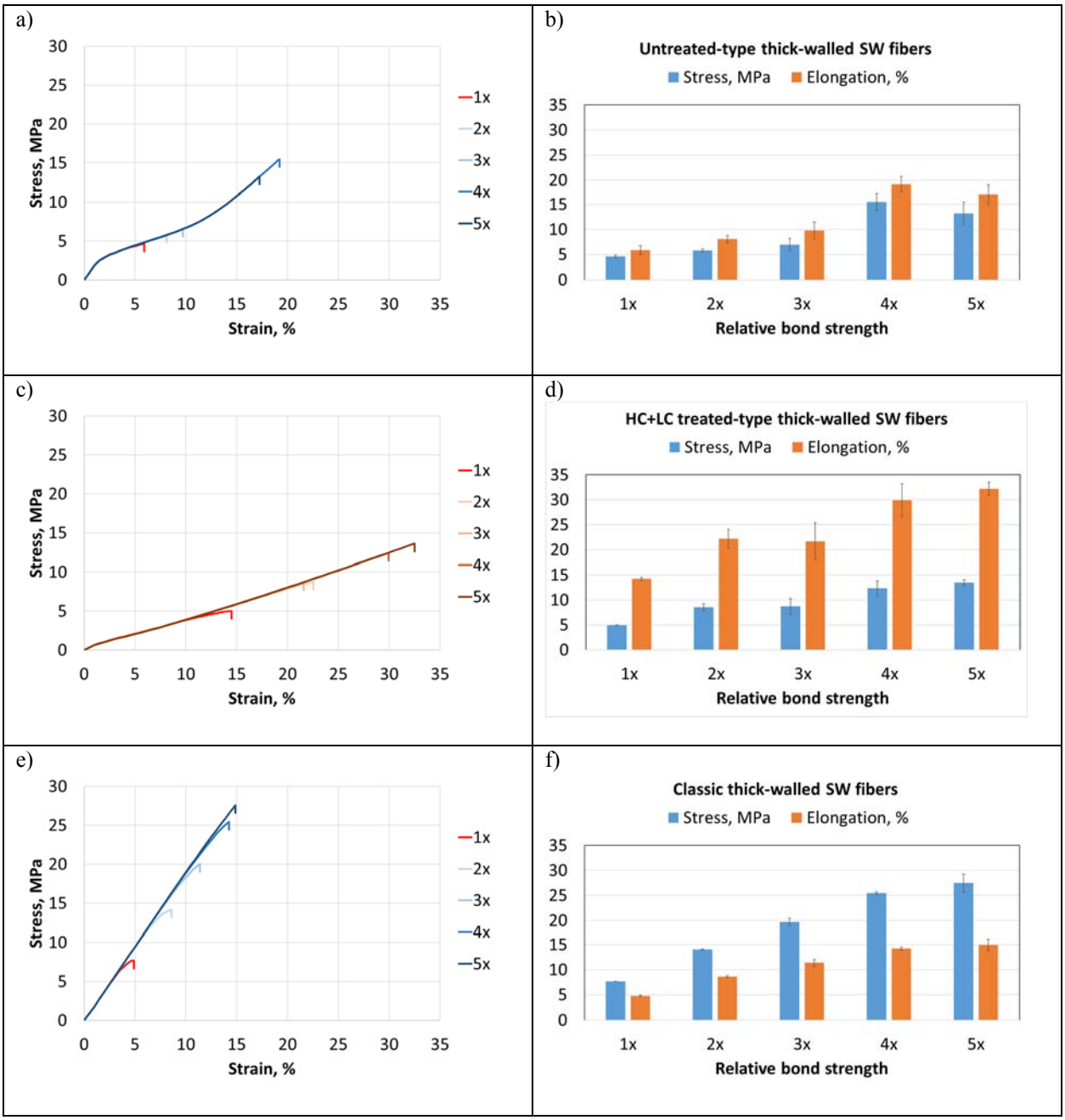

Fig. 6 Stress-strain curves representing the average strengths and elongations (left column) and average strength and elongation of the simulated fiber networks (right column): (a-b) unrefined thick-walled BSKP, (c-d) HC+LC refined thick-walled BSKP, (e-f) mimicked classic thick-walled SW fiber. Initial bond number was constant (100%) and bond strength was varied (the 1x value was 10.9 mN).

Although the strength of the network increases with increased bond strength initially, it dropped once the bond strength was increased by a factor of five (5x) with respect to the reference value (1x). As the failure of the network in the considered simulations can only be due to the de-bonding and the failure propagates through the network from the critical clusters, this result may suggest that releasing the energy gradually has an advantage over a situation when it is concentrated in isolated regions. This aspect should be explored in conjunction with the fiber failure mechanism, which has not yet been included in the simulations.

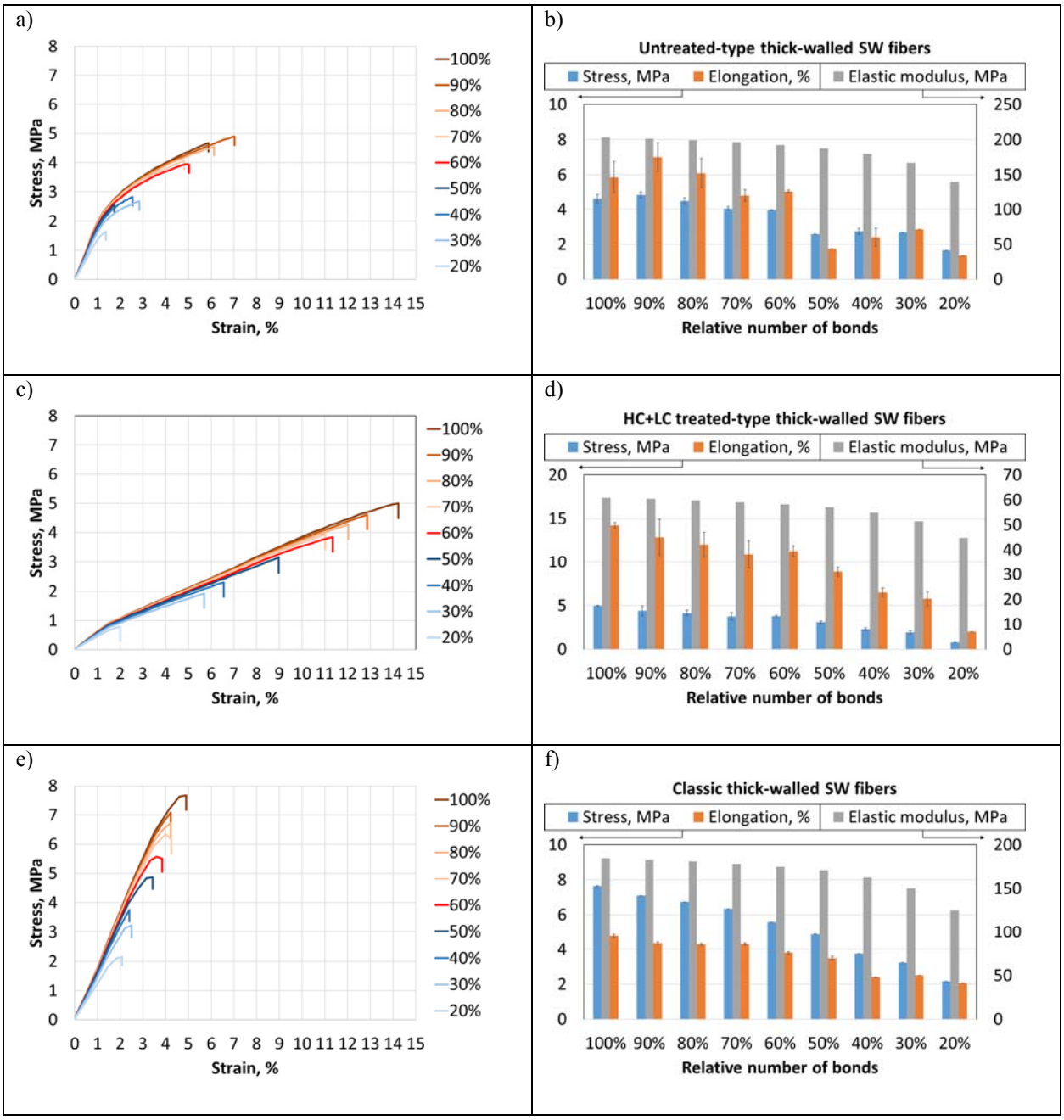

Fig. 7 Stress-strain curves representing the average strengths, elongations and elastic moduli (left column) and average strength and elongation of the simulated fiber networks (right column): (a-b) unrefined thick-walled BSKP, (c-d) HC+LC refined thick-walled BSKP, (e-f) mimicked classic thick-walled SW fiber. Initial bond number was varied and bond strength was constant (the 1x value 10.9 mN).

Influence of number of bonds. The stress-strain curves of simulated fiber networks with varied relative bond number for untreated-type, HC+LC treated-type and mimicked classic SW fibers are presented in Fig. 7 a, c, and e, respectively. Decrease of the relative bond number from the reference value (100%) clearly decreased strength, elongation and elastic modulus of all the simulated fiber networks, though in the case of untreated-type BSKP fiber the maximum strength and elongation was obtained with the relative bond number of 90%. The average strength, elongation and elastic modulus of the simulated fiber networks with 95% confidence limits are presented in Figs. 7 b, d, and f. The stress-strain curves of the simulated fiber networks of the untreated-type, HC+LC treated-type and mimicked classic SW fibers were clearly different, but in comparison to the stress-strain curves of actual handsheets (Fig. 7) similarities can be found in all cases. The stress-strain curves of the varied bond numbers did not fall on the same curves, but all the parallel repeats fell on the same curves with varied break points. Interestingly, variation of the stress-strain curves with limited variation of the relative bond numbers, e.g., from 70% to 100% resembled typical variation of tensile test repeats of actual paper samples. This simulation result indicates that activation of the fiber network is influenced by the number of bonds. The strength and elongation may have apparently linear correlation and both clearly depend on the extent of inter-fiber bonding.

In actual papers, bond number and strength of fiber contacts can be increased, e.g., by wet-pressing, refining and applying chemical additives, which can improve the strength of paper as shown in Fig. 4. The experimental results and simulations showed that fiber bonding has an important role, not only in determining the strength, but also the elongation of fiber networks, which is in accordance with Seth (2005) [1] and its references. On the other hand, the results indicate that the shape of stress-strain curve of individual pulp fibers may have significant influence on the shape of the stress-strain curve of a paper sheet. A large increase in the elongation and strength of a paper can only be reached by strengthening fiber-fiber bonding, as demonstrated by the handsheets with starch and CMF (Fig. 4 b) and by the fiber network simulations (Figs. 6 and 7). The result show that high elongation of paper can be promoted by enabling shrinkage of the fiber network and securing high bonding ability of fibers (Fig. 4). As a summary, unrestrained drying of BSKP fiber sheets in combination with increased fiber bond strength may be a promising approach for increasing paper extensibility.

CONCLUSION

BSKP fibers (Scots pine - Pinus Sylvestris - and Norway spruce - Picea Abies) were modified using a combination of high consistency and low consistency refining in order to increase sheet extensibility. The extensibility of the treated and untreated fibers was measured using single fiber tensile testing. Fiber network simulations were carried out to elucidate the effect of the change in fiber and bond properties on the tensile load behavior of the sheet. The stress-strain curves of two actual individual pulp fibers with relatively high strength 208 mN and 180 mN and high elongation 15% and 31% were applied to a micromechanical simulation of random fiber networks. Additionally, a linear mimicked stress-strain curve with strength 208 mN and elongation 5% was applied to the simulation.

The effect of fiber-fiber bond strength was studied experimentally by adding starch and CMF to the BSKP furnish, and in the fiber network simulations by increasing the fiber-fiber bond strength. In both handsheets and simulations this led to a strong increase in sheet strength and elongation. This leads to the conclusion that strong fiber-fiber bonding is highly relevant for sheet extensibility, only in a well bonded sheet can the full straining potential of the fibers be exploited. Comparison of the tensile tests of individual fibers and paper suggest that still only a part of the elongation potential of individual fibers can be utilized in the elongation of the investigated papers. The simulated uniform inter-fiber bond strength did not influence the shape of the stress-strain curve of fiber network until the bonds failed, whereas the number of bonds had an influence on the activation of the fiber network and varied shape of the stress-strain curve. On the other hand, the results indicate that the shape of the stress-strain curve of individual pulp fibers has an influence on the shape of stress-strain curve of a paper sheet. The experimental results show that high elongation of paper can be promoted by enabling shrinkage of the fiber network and securing the high bonding ability of fibers. The individual BSKP fiber elongation and stiffness were nearly doubled due to refining (from Untreated to HC+LC), whereas a slight decrease in fiber strength was observed. In the network simulations this led to a considerable drop in paper stiffness, which indicates a direct relation between fiber elongation and sheet elongation. Density increase in the handsheets, as a result of refining, compensated for the effect of the decreased mechanical properties of the fiber during refining.

The key conclusion related to this investigation was that the increased network elongation was created by two factors. First, increased bonding improved paper strength and thus increased the strain to break. Second, the role of free shrinkage was again shown to be pivotal for sheet extensibility.

ACKNOWLEDGEMENTS

This investigation was a part of the Academy of Finland's Flagship Programme under Projects No. 318890 and 318891 (Competence Center for Materials Bioeconomy, FinnCERES). The experimental investigation was funded by the ExtBioNet project supported by the Academy of Finland, the ACel program of the Finnish Bioeconomy Cluster CLIC Innovation and Association of European Fibre and Paper Research Organizations (EFPRO). Also, the financial support for the CD Laboratory from the Austrian Federal Ministry of Science, Research and Economy and the National Foundation for Research, Technology and Development is gratefully acknowledged. The authors wish to thank Dr. W.J. Fischer, Dr. M. Jajcinovic and M.Sc. A. Ketola for their contribution to the experimental investigation and to the preparation of the Journal article [23].

REFERENCES

1. Seth, R.S., "Understanding sheet extensibility," Pulp Paper Mag Can, 106(2):33-40 (2005).
2. Vishtal, A., Retulainen, E., "Boosting the extensibility potential of fiber networks: A review," Bioresources, 9(4):7951-8001 (2014).
3. Lindström, T., Wågberg, L., Larsson, T., "On the nature of joint strength in paper – a review of dry and wet strength resins used in paper," In Advances in paper science and technology, Trans. XIIIth Fund. Res. Symp. Oxford, (S.J. I'Anson, ed.), pp. 457–562 (2005).
4. Hubbe, M.A., "Prospects for Maintaining Strength of Paper and Paperboard Products While Using Less Forest Resources: A Review," Bioresources, 9(1):1634-1763 (2014).
5. Leopold, B., McIntosh, D.C., "Chemical Composition and Physical Properties of Wood Fibres. Tensile Strength of Individual Fibers From Alkali Extracted Loblolly Pine Holocellulose," Tappi, 44(3):235-240 (1961).
6. Jentzen, C.A., "The Effect of Stress Applied During Drying on some of the Properties of Individual Pulp Fibers," Tappi, 47(7):412-418 (1964).
7. Spiegelberg, H.L., "The effect of hemicelluloses on the mechanical properties of individual pulp fibers," Tappi, 49(9):388-396 (1966).
8. Hill, R.L., "The Creep Behavior of Individual Pulp Fibers Under Tensile Stress," Tappi, 56(8):432-440 (1967).
9. Alexander, S.D., Marton, R., McGovern, S.D., "Effect of beating and wet pressing on fiber and sheet properties. I. Individual fiber properties," Tappi, 51(6):277–283 (1968).
10. Hardacker, K.W., Brezinski, J.P., "The Individual Fiber Properties of Commercial Pulps," Tappi, 56(4):154-157 (1973).
11. Duncker, B., Nordman, L. "Determination of the strength of single fibres," Paperi Puu, 47(10):539-552 (1965).
12. Page, D.H., El-Hosseiny, F., Winkler, K., Bain, R., "The Mechanical Properties of Single Wood Pulp Fibres. I. A New Approach," Pulp Paper Mag Can, 73(8):T198-T203 (1972).
13. Page, D.H., Seth, R.S., "The elastic modulus of paper III: The effects of dislocation, microcompressions, curls, crimps and kinks," Tappi, 63(10):99-102 (1980).
14. Page, D.H., El-Hosseiny, F., "The mechanical properties of single wood pulp fibres. Part VI. Fibril angle and the shape of the stress-strain curve," J Pulp Pap Sci, 9(4):99-100 (1983).
15. Groom, L., Mott, L., Shaler, S., "Mechanical properties of individual Southern pine fibers. Part I. Determination and variability of stress-strain curves with respect to tree height and juvenility," Wood Fiber Sci, 34(1):14-27 (2002).
16. Jajcinovic, M., Fischer, W.J., Hirn, U., Bauer, W., "Strength of individual hardwood fibres and fibre to fibre joints," Cellulose, 23:2049–2060 (2016).
17. Jayme, B.A., "Mechanische Eigenschaften von Holzfasern," Tappi, 42(6):461–467 (1959).
18. Kallmes, O.J., Perez, M., "Load/elongation properties of fibres," In Consolidation of the Paper Web, Trans. IIIrd Fund. Res. Symp. Cambridge, pp. 507–528 (1965).
19. Kallmes, O.J., Perez, M., "A new theory for the load/elongation properties of paper," In Consolidation of the Paper Web, Trans. IIIrd Fund. Res. Symp. Cambridge, pp. 779–800 (1965).
20. Van den Akker, J.A., Jentzen, C.A., Spiegelberg, H.L., "Effects on individual fibres of drying under tension," In Consolidation of the Paper Web, Trans. IIIrd Fund. Res. Symp. Cambridge, pp. 477–506 (1965).
21. Leopold, B., "Effect of pulp processing on individual fiber strength," Tappi, 49(7):315-318 (1966).
22. Mott, L., Groom, L., Shaler, S., "Mechanical properties of individual Southern pine fibers. Part II. Comparison of earlywood and latewood fibers with respect to tree height and juvenility," Wood Fiber Sci 34(2):221-237 (2002).

23. Kouko, J., Jajcinovic, M., Fischer, W., Ketola, A., Hirn, U., Retulainen, E., "Effect of mechanically induced micro deformations on extensibility and strength of individual softwood pulp fibers and sheets," Cellulose 26(3):1995-2012 (2019).
24. Dumbleton, D.P., "Longitudinal Compression of Individual Fibers," Doctoral Thesis, The Institute of Paper Chemistry, Appleton, Wisconsin, (1971).
25. Hamad, W., Gurnagul, N., Gulati, D., "Analysis of fibre deformation processes in high-consistency refining based on Raman microscopy and x-ray diffraction," Holzforschung 66:711-716 (2012).
26. Hirn, U., Schennach, R., "Comprehensive analysis of individual pulp fiber bonds quantifies the mechanisms of fiber bonding in paper," Scientific Reports, 5:10503 (2015). DOI: 10.1038/srep105033
27. Motamedian, H.R., "Beam-to-Beam Contact and Its Application to Micromechanical Simulation of Fiber Networks," Doctoral thesis, KTH Royal Institute of Technology, 2018.
28. Borodulina, S., "Micromechanics of Fiber Networks," Doctoral thesis, KTH Royal Institute of Technology, 2016.
29. Kulachenko, A., Uesaka, T., "Direct simulations of fiber network deformation and failure," Mech Mater, 51: 1–14 (2012).
30. Khakalo, A., Vishtal, A., Retulainen, E., Filpponen, I., Rojas, O.J. "Mechanically-induced dimensional extensibility of fibers towards tough fiber networks," Cellulose 24:191-205 (2017).
31. Zeng, X., Vishtal, A., Retulainen, E., Sivonen, E., Fu, S., "The Elongation Potential of Paper How Should Fibres be Deformed to Make Paper Extensible?" Bioresources 8(1):472-486 (2013).
32. Kappel, L., Hirn, U., Bauer, W., Schennach, R., "A novel method for the determination of bonded area of individual fiber-fiber bonds," Nord Pulp Pap Res J, 24(2):199-205 (2009).
33. Lorbach, C., Fischer, W.J., Gregorova, A., Hirn, U., Bauer, W., "Pulp fiber bending stiffness in wet and dry state measured from moment of inertia and modulus of elasticity," Bioresources, 9(3):5511–5528 (2014).
34. Hardacker, K.W, "Effects of loading rate, span and beating on individual wood fiber tensile properties," In: The physics and chemistry of wood pulp fibers. D.H. Page (ed). Tappi Stap, 8:201-216 (1970).
35. Ilvessalo-Pläffli, M.S., "Fiber atlas: identification of papermaking fibers," Springer, Berlin, pp 33–163 (1995).
36. Fischer, W.J., Hirn, U., Bauer, W., Schennach, R., "Testing of individual fiber-fiber joints under biaxial load and simultaneous analysis of deformation," Nord Pulp Pap Res J, 27(2):237-244 (2012).
37. Borodulina, S., Motamedian H. R., Kulachenko A., "Effect of fiber and bond strength variations on the tensile stiffness and strength of fiber networks," Int J Solids Struct, 154(1):19-32 (2018).
38. Kulachenko, A., Uesaka, T., "Direct simulations of fiber network deformation and failure," Mech Mater., 51:1-14 (2012).
39. Motamedian, H. R., Kulachenko, A., "Rotational Constraint between Beams in 3-D Space," Mech Sci, 9(2):373-387 (2018).
40. Borodulina, S., Kulachenko, A., Tjahjanto, D.D., "Constitutive modeling of a paper fiber in cyclic loading applications," Comput Mater Sci 110:227–240 (2015).
41. Fischer, W.J., Zankel, A., Ganser, C., Schmied, F.J., Schroettner, H., Hirn, U., Teichert, C., Bauer, W., Schennach, R., "Imaging of the formerly bonded area of individual fibre to fibre joints with SEM and AFM," Cellulose, 21:251–260 (2014). DOI 10.1007/s10570-013-0107-0
42. Sormunen, T., Ketola, A., Miettinen, A., Parkkonen, J., Retulainen, E., "X-Ray Nanotomography of Individual Pulp Fibre Bonds Reveals the Effect of Wall Thickness on Contact Area," Sci Rep, 9:4258 (2019).
43. Yiannos, P.N., "The apparent cell-wall density of wood and pulp fibers," Tappi, 47(8):468-471 (1964).
44. Janes, R.L., "Fiber characteristics," Tappi Notes, (1992).
45. Zeng, X., Retulainen, E., Heinemann, S., Fu, S., "Fibre deformations induced by different mechanical treatments and their effect on zero-span strength," Nord Pulp Pap Res J, 27(2):335-342 (2012).
46. Seth, R.J., Page, D.H., "The stress-strain curve of paper," In The role of fundamental research in paper making, Trans. VIIth Fund. Res. Symp. Cambridge, pp. 421–452 (1981).
47. Borodulina, S., Kulachenko, A., Nygårds, M., Galland, S., "Stress-strain curve of paper revisited," Nordic Pulp Pap Res J, 27(2):318-328 (2012).
48. Magnusson, M.S., Zhang, X., Östlund, S., "Experimental Evaluation of the Interfibre Joint Strength of Papermaking Fibres in Terms of Manufacturing Parameters and in Two Different Loading Directions," Exp Mech 53(9):1621–1634 (2013).
49. Borodulina, S., Motamedian, H.R., Kulachenko, A., "Effect of fiber and bond strength variations on the tensile stiffness and strength of fiber networks," Int J Solids Struct, 154:19-32 (2016).
50. Davison, R.W., "The Weak Link in Paper Dry Strength," Tappi, 55(4):567-573 (1972).
51. Retulainen, E., Niskanen, K., Nilsen, N., "Fibers and bonds," In Paper Physics, (K. Niskanen, ed.), Fapet Oy, Helsinki, Finland, pp. 55–87 (1998).